

## Comparison of the LES subgrid-scale models in simulating the turbulent channel flow

Seokwon Whang<sup>a</sup>, Ralph Carlo Evidente<sup>a</sup>, Hyun Sun Park<sup>a\*</sup>

<sup>a</sup>Division of Advance Nuclear Engineering, POSTECH, Pohang, Gyeongbuk 37673, Republic of Korea

\*Corresponding author: hejsunny@postech.ac.kr

### 1. Introduction

IVR-ERVC is one of the severe accident management strategies to prevent RPV from failure. The integrity of RPV is determined by comparing the internal heat flux with the external critical heat flux. For the realistic assessment, it is important to accurately predict the internal heat flux, i.e. thermal behavior of molten pool materials so called corium. One of the key phenomena determining the corium behaviors is a turbulent natural convection generated by the internal decay heat generation. Although some experiments have been conducted using simulants, experiments under real conditions have not been carried out.

It has been reported that the thermal-hydraulic behavior can be changed depending on the material even in the same condition such as Rayleigh or Grashof number [1, 2]. Especially, the upward heat transfer rate of oxide layer under certain condition increases due to the above-mentioned phenomena [3]. However, the RANS model used in that study was validated with water data, not the corium one. Therefore, a high-fidelity simulation such as LES is required to accurately investigate the effect of the material properties on the thermal behavior in the oxide layer.

LES becomes popular as a numerical experiment in conditions where experiments cannot be performed. The adequacy of LES results largely depends on the sub-grid scale (SGS) model. Therefore, in this paper, the applicability of LES analysis in the turbulent natural convection of the corium pool will be examined by testing SGS models in a simple geometry. For the SGS models, the dynamic Vreman model, one of the representative SGS models, is selected to simulate turbulent natural convection [4]. Unlike the typical SGS models in which model coefficients are defined by users, the dynamic model calculates model coefficients in terms of flow conditions.

In this study, various SGS models including the dynamic Vreman model are compared in a simple geometry such as a channel flow with or without uniform heating to explore the model validity. The simulation selected for the tests are as follows: the channel flow ( $Re_\tau = 180$  and  $395$ ), the channel flow with uniform heat flux along the wall ( $Re_\tau = 180$  and  $395$ ;  $Pr = 0.025, 0.71, 7$ ).

### 2. Methodology

#### 2.1. Governing equations

The filtered Navier–Stokes (NS) equations are solved for simulating the incompressible turbulent flows:

$$\frac{\partial \bar{u}_i}{\partial x_i} = 0 \quad (1)$$

$$\frac{\partial \bar{u}_i}{\partial t} + \frac{\partial \bar{u}_i \bar{u}_j}{\partial x_j} = -\frac{1}{\rho} \frac{\partial \bar{p}}{\partial x_i} + \nu \frac{\partial^2 \bar{u}_i}{\partial x_j \partial x_j} - \frac{\partial \tau_{ij}}{\partial x_j} \quad (2)$$

where the  $\bar{u}_i$  and  $\bar{p}$  denote the filtered velocity and pressure, respectively,  $\nu$  is the kinematic viscosity and  $\tau_{ij}$  is the SGS stress tensor. The SGS stress tensor can be modelled with the eddy-viscosity assumption:

$$\tau_{ij} - \frac{1}{3} \tau_{kk} \delta_{ij} = -2\nu_T \bar{S}_{ij} \quad (3)$$

where the  $\nu_T$  is the eddy viscosity.

#### 2.2. Dynamic Vreman model

In the Vreman-type model, the eddy viscosity is proposed to be:

$$\nu_T = C_v \Pi^g,$$

$$\Pi^g = \sqrt{\frac{B_\beta^g}{\alpha_{kl} \alpha_{kl}}}$$

$$B_\beta^g = \beta_{11}^g \beta_{22}^g - \beta_{12}^g \beta_{12}^g + \beta_{11}^g \beta_{33}^g - \beta_{13}^g \beta_{13}^g + \beta_{22}^g \beta_{22}^g - \beta_{23}^g \beta_{23}^g, \quad (4)$$

$$\beta_{ij}^g = \sum_{m=1}^3 \Delta_m \alpha_{mi} \alpha_{mj},$$

$$\alpha_{ij} = \frac{\partial \bar{u}_j}{\partial x_i}$$

$C_v$  is set to be 0.07 in homogeneous turbulent flow [5]. However, You and Moin [4] suggest dynamic model based on the global-equilibrium assumption:

$$C_v = -\frac{\nu}{2} \frac{\overline{\langle \alpha_{ij} \alpha_{ij} - \alpha_{ij} \alpha_{ij} \rangle}}{\overline{\langle \Pi^g S_{ij} S_{ij} - \Pi^g S_{ij} S_{ij} \rangle}} \quad (5)$$

where  $S_{ij}$  is strain rate tensor and  $\Pi_i$  is defined in Eq. (4) with additional filtered elements. Here, the model coefficient is a single value in space, but is to vary in time.

### 2.3 Channel flow

In this study, we validate the SGS model in turbulent channel flow that is a theoretical flow between two infinite parallel planes, driven by a constant pressure gradient as shown in Fig. 1. Computational channel size and numerical condition are listed in Table I. The bulk velocity and bulk Reynolds number in Table I are provided when the  $Re_\tau$  is 395 [6].

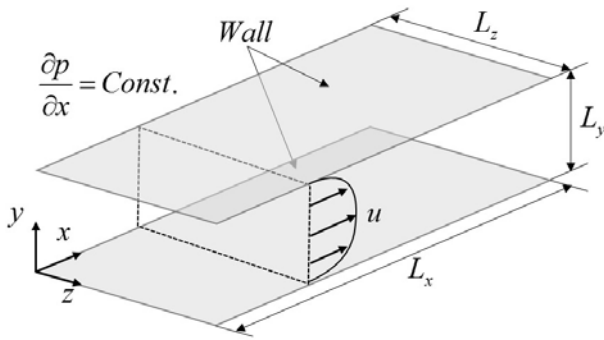


Fig. 1. Computational domain for channel flow

Table I: Physical and geometrical parameters for channel flow

Channel quantity	Value
Height, $L_y$ (m)	2
Streamwise length, $L_x$ (m)	6
Spanwise length, $L_z$ (m)	3
Kinematic viscosity ( $m^2/s$ )	$2 \times 10^{-5}$
Bulk velocity (m/s)	0.1335
$Re_b$	13,350

### 2.4 Numerical methods

In this study, the calculation is conducted with OpenFOAM and the ‘pimpleFoam’ solver is used to solve the incompressible Navier–Stokes equations. In this study, Smagorinsky (SM), dynamic Smagorinsky (DSM), Vreman (VM) and dynamic Vreman model (DVM) are implemented in the code. A backward differencing scheme was used for time marching, Gauss linear and linear central differencing (second order) were applied for the gradient and divergence, respectively. In the simulation, Courant number and  $y^+$  are less than 1 by adjusting time step and grid size. The number of grid for the channel flow is 0.15M ( $48 \times 66 \times 48$ ).

## 3. Results

The calculation is currently in progress, and the following is the preliminary analysis result comparing the VM and DVM. The DNS data from Kawamura et al. [7] is used as references.

Figure 2 shows the mean velocity profiles for different SGS models at  $Re_\tau = 395$ . Generally, the results from DSM, VM and DVM are in good agreement with that from DNS data. The simulation with SM significantly underestimates than DNS.

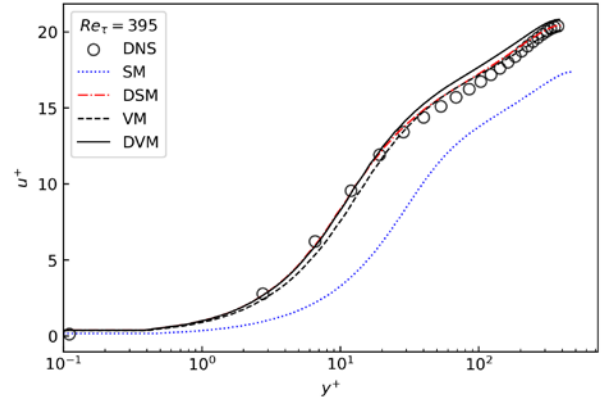


Figure 2. Profiles of the mean streamwise velocity in turbulent channel flows at  $Re_\tau = 395$ .

Figure 3 shows the stress tensor component describing turbulent fluctuation. Standard deviation of root mean square (rms) of velocity component in each direction is illustrated. Except SM case, the overall behavior is similar with DNS data. The maximum value near the wall tended to be overestimated ( $u_{rms}^+$ ) or underestimated ( $v_{rms}^+$ ,  $w_{rms}^+$ ). The predicted values of bulk were less than the DNS.

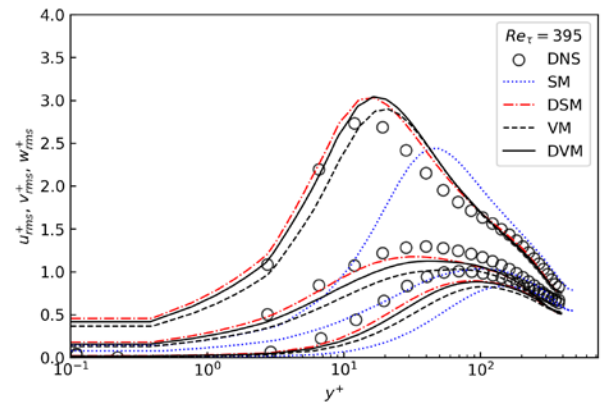


Figure 3. Profiles of the rms velocity fluctuations in turbulent channel flows at  $Re_\tau = 395$ .

Figure 4 and 5 show mean temperature and temperature fluctuation in turbulent channel flow with uniform heat flux along the wall. In this study, three Prandtl number cases were compared; 0.025, 0.71 and 7.0, respectively. Except low Prandtl number case, the SM

underestimated mean temperature and predicted different tendency in temperature fluctuation. In this study, it can be observed that the dynamic-models (DSM and DVM) are good at predicting results.

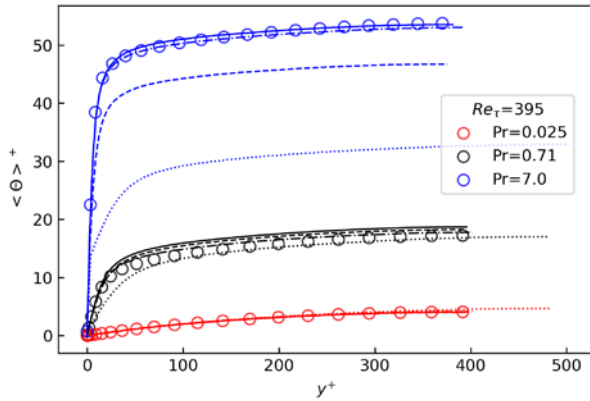


Figure 4. Profiles of the mean temperature in turbulent channel flows with uniform heat flux at  $Re_{\tau} = 395$ . Dotted line, SM; chain-dotted line, DSM; dashed line, VM; solid line, DVM.

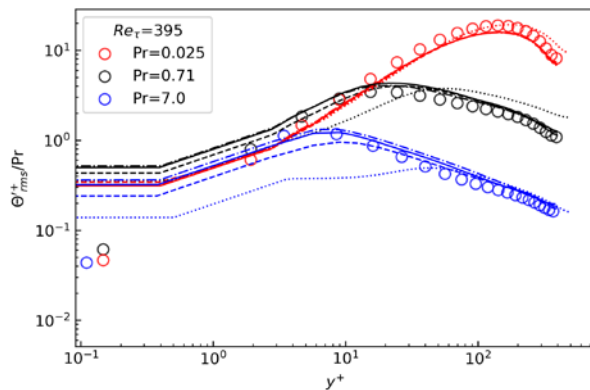


Figure 5. Profiles of the rms temperature fluctuations in turbulent channel flows with uniform heat flux at  $Re_{\tau} = 395$ . Dotted line, SM; chain-dotted line, DSM; dashed line, VM; solid line, DVM.

#### 4. Conclusion

In this study, the performance of different LES SGS models are evaluated in the turbulent channel flow with or without uniform heat flux along the wall. The dynamic-models, especially dynamic Vreman model shows the best agreement with the DNS among other SGS models. Currently, model validation in turbulent natural convection flow is underway. Once model validation of turbulent natural convection flow has been completed, it is expected that the model (DVM) will also be applicable to simulate oxidation layer phenomena, i.e. turbulent natural convection flow with internal heating.

#### Acknowledgement

This work was supported by KOREA HYDRO & NUCLEAR POWER CO., LTD (No. Safety 2-1, "High-Fidelity Numerical Analysis of Highly Turbulent Corium Pool for In-Vessel Retention (IVR) Strategy Feasibility Assessment")

#### REFERENCES

- [1] J.D. Scheel, J. Schumacher, Global and local statistics in turbulent convection at low Prandtl numbers. *Journal of Fluid Mechanics*, 2016.
- [2] R.R. Nourgaliev, T.N. Dinh, B.R. Sehgal, Effect of fluid Prandtl number on heat transfer characteristics in internally heated liquid pools with Rayleigh numbers up to 10(12). *Nuclear Engineering and Design*, Vol.169, p.165–184, 1997.
- [3] S. Whang, H.S. Park, K. Lim, Y.J. Cho, Prandtl number effect on thermal behavior in volumetrically heated pool in the high Rayleigh number region. *Nuclear Engineering and Design*, Vol.351, p.72–79, 2019.
- [4] D. You, P. Moin, A dynamic global-coefficient subgrid-scale eddy-viscosity model for large-eddy simulation in complex geometries. *Phys. Fluids*, 2007.
- [5] A.W. Vreman, An eddy-viscosity subgrid-scale model for turbulent shear flow: Algebraic theory and applications. *Phys. Fluids*, 2004.
- [6] E. De Villiers, The Potential of Large Eddy Simulation for the Modeling of Wall Bounded Flows, Ph.D. thesis, The Imperial College of Science, Technology and Medicine, 2006.
- [7] H. Kawamura, K. Ohsaka, H. Abe, K. Yamamoto, DNS of turbulent heat transfer in channel flow with low to medium-high Prandtl number fluid, *International Journal of Heat and Fluid Flow*, 1998.